Asian Journal of Chemistry; Vol. 38, No. 8 (2026), 2102-2108
ASIAN JOURNAL OF CHEMISTRY
https://doi.org/10.14233/ajchem.2026.36108

Piperazine-Pyrrolidone Acyl Hydrazide Hybrids as New Anticancer Agents against Breast Cancer

DILEEP NAGARAJU[1], MAMATHA S. KEMPASIDDEGOWDA[2], MAHESHA KUMARASWAMY[3], BHOOMIKA B. RAVI[1], H.S. MONISHA YADAV[1], TORESHETTAHALLY R. SWAROOP[1], SANTOSH L. GOANKAR[4] and BASAPPA BASAPPA[1,*]

[1]Department of Studies in Organic Chemistry, University of Mysore, Manasagangotri, Mysuru-570006, India
[2]Tsinghua-Berkeley Shenzhen Institute and The Institute of Biopharmaceutical and Health Engineering, Tsinghua Shenzhen International Graduate School, Tsinghua University, Shenzhen-518055, People's Republic of China
[3]Department of Chemistry, Sri Mahadeshwara Government First Grade College, Kollegala-571440, India
[4]Department of Chemistry, Manipal Institute of Technology, Manipal Academy of Higher Education, Manipal-576104, India

*Corresponding author: E-mail: salundibasappa@gmail.com

Received: 31 March 2026 *Accepted*: 2 July 2026 *Published online*: 7 August 2026 AJC-22436

Present work describes the development and evaluation of novel piperazine–pyrrolidone acyl hydrazide hybrids as potential anticancer agents for breast cancer treatment. The cytotoxic activities of these compounds were determined against human breast cancer cell lines (MCF-7) by alamar blue assay. A compound 1-(4-(4-chloro-2-fluorophenyl)piperazin-1-yl)-5-oxopyrrolidine-3-carbohydrazide (**7b**) showed the highest cytotoxicity with IC_{50} value of 1.46 μM. The lead candidate exhibited superior activity compared to the standard drug tamoxifen (1.75 μM) and was approximately two-fold less potent than doxorubicin (0.73 μM). A structure–activity relationship (SAR) analysis was carried out to understand the effect of structural modifications on anticancer activity. The findings suggest that the lead molecule induces apoptosis in cancer cells by inhibiting the interaction between BCL-XL and BAD, a mechanism supported by *in silico* studies.

Keywords: Piperazine, Pyrrolidone, Acyl hydrazide, Anticancer, Breast cancer, Cytotoxic, Docking studies.

INTRODUCTION

Piperazine exhibits diverse pharmacological properties [1], while the presence of nitrogen atoms at the 1- and 4-positions contributes to improve the specificity, affinity, water solubility, bioavailability, molecular rigidity, hydrogen-bonding capacity and polar surface area. In addition, piperazine also demonstrates strong anticancer activities [2]. Several anticancer drugs such as olaparib, ponatinib, dasatinib, bosutinib, abemaciclib, venetoclax, palbociclib, brigatinib and imatinib contain piperazine moiety. On the other hand, 2-pyrrolidone derivatives have attracted considerable interest owing to their notable anticancer properties [3] and this moiety is present in several anticancer agents such as sunitinib, semaxanib, toceranib and SU6668. Finally, acyl hydrazide derivatives have shown promising anticancer activity [4]. Several anticancer agents containing this pharmacophore such as aldoxorubicin, PAC-1 and LASSBio-294, have progressed to clinical evaluation. The occurrence of piperazine, pyrrolidone and acyl hydrazide motifs in anticancer drugs motivated the design and synthesis of new hybrid molecules incorporating these structural features with the aim of improving anticancer activity. To the best of our knowledge, such piperazine-pyrrolidone acyl hydrazide hybrids have not been evaluated against cancer models. In medicinal chemistry, the combination of privileged scaffolds is often associated with improved physico-chemical and pharmacological properties such as bioavailability, lipophilicity and target-binding affinity [5].

The anti-apoptotic protein BCL-XL plays an important role in cancer cell survival by binding to the pro-apoptotic protein BAD and preventing activation of the apoptotic pathway. This interaction occurs at the hydrophobic binding groove of BCL-XL and inhibits downstream apoptotic signaling. Disruption of the BCL-XL/BAD protein–protein interaction has emerged as a promising strategy for restoring apoptosis in cancer cells. Small molecules capable of occupying the BCL-XL binding groove can block this interaction and promote apoptotic cell death, thereby suppressing tumour growth

[6]. In the present study, molecular docking studies against BCL-XL were carried out to investigate the possible mode of action of the designed compounds.

As part of ongoing efforts in synthetic organic chemistry [7-9] and medicinal chemistry [10,11], several anticancer agents have already been developed [12,13]. This work led to the design and synthesis of piperazine–pyrrolidone–acyl hydrazide hybrids as potential anticancer agents targeting BCL-XL.

EXPERIMENTAL

All reagents, chemicals and solvents were purchased from SD Fine Chem, Rankem and Sigma-Aldrich, India. Thin-layer chromatography (TLC) was used to monitor the progress of reactions. Melting points were determined using Selaco melting point apparatus and are uncorrected. IR spectra were obtained from Perkin-Elmer spectrometer. NMR spectra were recorded using DMSO-d_6 as solvent and tetramethylsilane as internal standard on Bruker WH-200 (400 MHz) spectrometer. High-resolution mass spectra were measured from Bruker Daltonics equipment.

Synthesis of 1-(4-chlorophenyl)-5-oxopyrrolidine-3-carboxylic acid (3): A mixture of itaconic acid (5 mmol) and *p*-chloroaniline (7.5 mmol) were heated at 90 ºC for 2 h. Upon completion of the reaction, the mixture was cooled to room temperature and treated with freshly prepared 2 N NaOH solution to ensure complete dissolution. The alkaline solution was then acidified by the gradual addition of HCl until neutral pH was reached, resulting in the formation of a precipitate. The precipitated solid was collected by filtration, washed thoroughly with distilled water and dried under reduced pressure to obtain compound **3**.

Synthesis of ethyl 1-(4-chlorophenyl)-5-oxopyrrolidine-3-carboxylate (4): Compound **3** (4 mmol) was treated with conc. H_2SO_4 (5 mL) in ethanol (20 mL) and the reaction mixture was heated at 80 ºC for 6 h. The progress of the reaction was monitored by TLC. After completion, the reaction mixture was allowed to cool to room temperature. The resulting solid was collected by filtration, washed with cold ethanol and dried under reduced pressure to afford compound **4**.

Synthesis of 1-(4-chlorophenyl)-5-oxopyrrolidine-3-carbohydrazide (5): Compound **4** (3 mmol) was reacted with hydrazine hydrate (12 mmol) in ethanol (10 mL) at 80 ºC for 6 h. The progress of the reaction was monitored by TLC and upon completion, the reaction mixture was cooled to room temperature. The resulting solid was washed thoroughly with water, collected by filtration and dried under reduced pressure to obtain compound **5**.

General procedure for the synthesis of 5-oxo-1-(4-(4-phenylpiperazin-1-yl)aryl)pyrrolidine-3-carbohydrazide derivatives (7a-f): The synthesised compound **5** (1 mmol) was reacted with various substituted piperazine **6** (1 mmol) in 1,4-dioxane (2 mL) at 100 ºC in the presence of PS-Co(BBZN)Cl_2 (12 mol%), BINAP (15 mol%) and Cs_2CO_3 (3 mmol) under N_2 atmosphere for about 8-10 h to afford the corresponding compounds **7**. The progress of the reaction was monitored by TLC. Upon completion, the reaction mixture was diluted with water and extracted with ethyl acetate. The organic layer was separated, dried under reduced pressure and concentrated to obtain the crude product (**Scheme-I**). Subsequent recrystallisation furnished the pure title compounds **7a-f** .

1-(4-(4-(4-Chlorophenyl)piperazin-1-yl)phenyl)-5-oxopyrrolidine-3-carbohydrazide (7a): White solid; yield: 83%; m.p.: 130-132 ºC; IR (neat, ν_{max}, cm^{-1}): 3305, 2993, 1660, 1595, 1326; ^{1}H NMR (400 MHz, DMSO-d_6, δ ppm): 9.37 (s, 1H, NH), 7.73 (d, *J* = 8.0 Hz, 2H, Ar-H), 7.46 (d, *J* = 8.0 Hz, 2H, Ar-H), 7.26 (d, *J* = 8.0 Hz, 2H, Ar-H), 6.96 (d, *J* = 8.0 Hz, 2H, Ar-H), 4.10 (s, 2H, NH_2), 4.00 (d, *J* = 8.0 Hz, 1H, CH), 3.87 (dd, *J* = 8.0, 2.0 Hz, 1H, CH), 3.09 (s, 8H, $(CH_2)_4$), 2.77 (dd, *J* = 8.0, 6.0 Hz, 2H, CH_2), 2.67 (dd, *J* = 8.0, 2.0 Hz, 1H, CH); HRMS (ESI) *m/z*: calcd. for $C_{21}H_{24}ClN_5O_2$ $[M + H]^+$ 414.1697; found, 414.1699.

1-(4-(4-(4-Chloro-2-fluorophenyl)piperazin-1-yl)-phenyl)-5-oxopyrrolidine-3-carbohydrazide (7b): White solid;

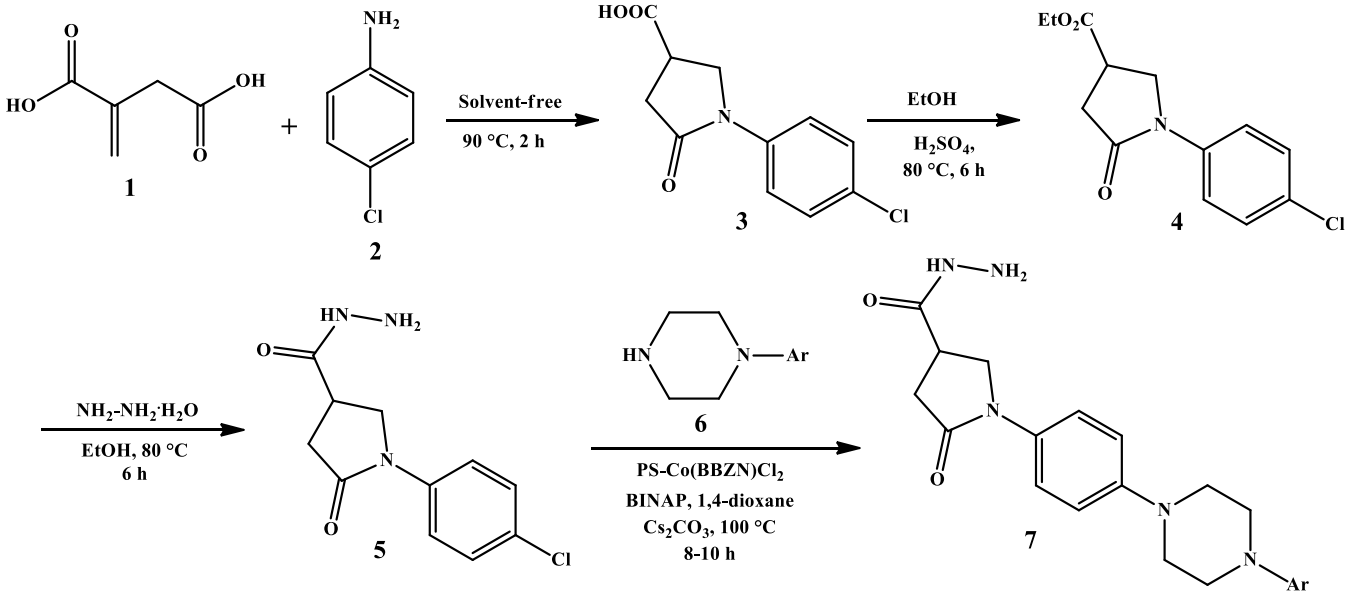

Scheme-I: Synthesis of piperazine–pyrrolidone acyl hydrazide hybrids

yield: 80%; m.p.: 144-146 ºC; IR (neat, ν_{max}, cm^{-1}): 3308, 2991, 1664, 1598, 1329; ^{1}H NMR (400 MHz, DMSO-d_6, δ ppm): 9.35 (s, 1H, NH), 7.73 (d, *J* = 8.0 Hz, 2H, Ar-H), 7.46 (d, *J* = 8.0 Hz, 2H, Ar-H), 7.35 (d, *J* = 8.0 Hz, 1H, Ar-H), 7.21 (d, *J* = 8.0 Hz, 1H, Ar-H), 7.07 (t, *J* = 8.0 Hz, 1H, Ar-H), 4.17 (s, 2H, NH_2), 4.02 (d, *J* = 8.0 Hz, 1H, CH), 3.88 (dd, *J* = 8.0, 6.0 Hz, 1H, CH), 2.96 (s, 8H, $(CH_2)_4$), 2.77 (dd, *J* = 8.0, 6.0 Hz, 2H, CH_2), 2.69 (d, *J* = 8.0 Hz, 1H, CH); HRMS (ESI) *m/z*: calcd. for $C_{21}H_{23}ClFN_5O_2$ $[M + H]^+$ 432.1603; found, 432.1606.

1-(4-(4-(2-Fluorophenyl)piperazin-1-yl)phenyl)-5-oxopyrrolidine-3-carbohydrazide (7c): White solid; yield: 78%; m.p.: 154-156 ºC; IR (neat, ν_{max}, cm^{-1}): 3310, 2988, 1668, 1591, 1331; ^{1}H NMR (400 MHz, DMSO-d_6, δ ppm): 8.07 (s, 1H, NH), 7.70 (s, 1H, Ar-H), 7.42 (d, *J* = 6.0 Hz, 1H, Ar-H), 7.11 (d, *J* = 7.2 Hz, 2H, Ar-H), 7.06-6.93 (m, 4H, Ar-H), 3.84 (s, 2H, NH_2), 3.59-3.48 (m, 2H, CH_2), 3.00 (s, 8H, $(CH_2)_4$), 2.61 (s, 2H, CH_2), 2.51 (s, 1H, CH); HRMS (ESI) *m/z*: calcd. for $C_{21}H_{24}FN_5O_2$ $[M + H]^+$ 398.1992; found, 398.1990.

1-(4-(4-(2-Nitrophenyl)piperazin-1-yl)phenyl)-5-oxopyrrolidine-3-carbohydrazide (7d): Brown solid; yield: 78%; m.p.: 144-146 ºC; IR (neat, ν_{max}, cm^{-1}): 3303, 2985, 1670, 1595, 1342; ^{1}H NMR (400 MHz, DMSO-d_6, δ ppm): 9.35 (s, 1H, NH), 7.82 (d, *J* = 7.0 Hz, 1H, Ar-H), 7.78-7.70 (m, 2H, Ar-H), 7.61 (dd, *J* = 8.0, 4.2 Hz, 1H, Ar-H), 7.47 (dd, *J* = 8.0, 4.0 Hz, 2H, Ar-H), 7.32 (d, *J* = 8.0 Hz, 1H, Ar-H), 7.14 (t, *J* = 7.8 Hz, 1H, Ar-H), 4.16-3.96 (m, 2H, NH_2), 3.62 (s, 8H, $(CH_2)_4$), 2.94 (d, *J* = 5.0 Hz, 2H, CH_2), 2.85 (d, *J* = 2.8 Hz, 2H, CH_2), 2.55 (s, 1H, CH); HRMS (ESI) *m/z*: calcd. for $C_{21}H_{24}N_6O_4$ $[M + H]^+$ 425.1937; found, 425.1934.

5-Oxo-1-(4-(4-(*p*-tolyl)piperazin-1-yl)phenyl)pyrrolidine-3-carbohydrazide (7e): White solid; yield: 85%; m.p.: 146-148 ºC; IR (neat, ν_{max}, cm^{-1}): 3301, 2984, 1668, 1598, 1336; ^{1}H NMR (400 MHz, DMSO-d_6, δ ppm): 7.73 (d, *J* = 8.0 Hz, 1H, Ar-H), 7.46 (d, *J* = 8.0 Hz, 1H, Ar-H), 7.06 (d, *J* = 8.0 Hz, 3H, Ar-H), 6.86 (d, *J* = 8.0 Hz, 3H, Ar-H), 4.22 (s, 2H, NH_2), 4.01 (t, *J* = 8.0 Hz, 1H, CH), 3.87 (dd, *J* = 8.0, 6.1 Hz, 1H, CH), 3.03 (s, 8H, $(CH_2)_4$), 2.86-2.72 (m, 2H, CH_2), 2.54 (s, 1H, CH), 2.23 (s, 3H, CH_3); HRMS (ESI) *m/z*: calcd. for $C_{22}H_{27}N_5O_2$ $[M + H]^+$ 394.2243; found, 394.2247.

5-Oxo-1-(4-(4-phenylpiperazin-1-yl)phenyl)pyrrolidine-3-carbohydrazide (7f): White solid; yield: 81%; m.p.: 134-136 ºC; IR (neat, ν_{max}, cm^{-1}): 3304, 2983, 1662, 1600, 1337; ^{1}H NMR (400 MHz, DMSO-d_6, δ ppm): 9.29 (s, 1H, NH), 7.69 (d, *J* = 8.4 Hz, 4H, Ar-H), 7.43 (d, *J* = 8.3 Hz, 5H, Ar-H), 4.33 (s, 2H, NH_2), 3.98 (t, *J* = 8.0 Hz, 1H, CH), 3.85-3.81 (m, 1H, CH), 3.36 (s, 8H, $(CH_2)_4$), 2.73 (dd, *J* = 8.0, 6.1 Hz, 2H, CH_2), 2.51 (s, 1H, CH); HRMS (ESI) *m/z*: calcd. for $C_{21}H_{25}N_5O_2$ $[M + H]^+$ 380.2087; found, 380.2084.

Synthesis of 1-(3-chlorophenyl)-5-oxopyrrolidine-3-carboxylic acid (9): A mixture of itaconic acid (5 mmol) and *m*-chloroaniline (7.5 mmol) were heated at 90 ºC for 2 h and upon completion of the reaction, the mixture was cooled to room temperature and treated with freshly prepared 2 N NaOH solution to ensure complete dissolution. The alkaline solution was then acidified by the gradual addition of HCl until neutral pH was reached, resulting in the formation of a precipitate. The precipitated solid was collected by filtration, washed thoroughly with distilled water and dried under reduced pressure to obtain compound **9**.

Synthesis of ethyl 1-(3-chlorophenyl)-5-oxopyrrolidine-3-carboxylate (10): Compound **9** (4 mmol) was treated with conc. H_2SO_4 (5 mL) in ethanol (20 mL) and the reaction mixture was heated at 80 ºC for 6 h. The progress of the reaction was monitored by TLC. After completion, the reaction mixture was allowed to cool to room temperature. The resulting solid was collected by filtration, washed with cold ethanol and dried under reduced pressure to afford compound **10**.

Synthesis of 1-(3-chlorophenyl)-5-oxopyrrolidine-3-carbohydrazide (11): Compound **10** (3 mmol) was reacted with hydrazine hydrate (12 mmol) in ethanol (10 mL) at 80 ºC for 6 h. The progress of the reaction was monitored using TLC. After completion of the reaction, the mixture was allowed to cool to ambient temperature and then the obtained precipitated solid was separated by filtration, washed thoroughly with water to remove impurities and dried under reduced pressure to afford compound **11** as the final product.

General procedure for the synthesis of 5-oxo-1-(4-(4-phenylpiperazin-1-yl)aryl)pyrrolidine-3-carbohydrazide derivatives (12a-d): Compound **11** (1 mmol) was reacted with various substituted piperazine **6** (1 mmol) in 1,4-dioxane (2 mL) at 100 ºC in the presence of PS-Co(BBZN)Cl_2 (12 mol%), BINAP (15 mol%) and Cs_2CO_3 (3 mmol) under N_2 atmosphere for about 8-10 h to afford the corresponding compound **12a-d**. The progress of the reaction was monitored by TLC. Upon completion, the reaction mixture was diluted with water and extracted with ethyl acetate. The organic layer was separated, dried under reduced pressure and concentrated to obtain the crude product. Subsequent recrystallisation furnished the pure title compounds **12a-d** (**Scheme-II**).

1-(3-(4-(4-Chlorophenyl)piperazin-1-yl)phenyl)-5-oxopyrrolidine-3-carbohydrazide (12a): White solid; yield: 75%; m.p.: 140-142 ºC; IR (neat, ν_{max}, cm^{-1}): 3301, 2980, 1666, 1602, 1342; ^{1}H NMR (400 MHz, DMSO-d_6, δ ppm): 10.33 (s, 1H, NH), 7.88 (s, 1H, Ar-H), 7.21 (d, *J* = 8.0 Hz, 4H, Ar-H), 6.90 (d, *J* = 8.0 Hz, 3H, Ar-H), 3.66 (s, 2H, NH_2), 3.03 (s, 8H, $(CH_2)_4$), 2.83 (d, *J* = 3.2 Hz, 2H, CH_2), 2.79-2.70 (m, 2H, CH_2), 2.70-2.63 (m, 1H, CH); HRMS (ESI) *m/z*: calcd. for $C_{21}H_{24}ClN_5O_2$ $[M + H]^+$ 414.1697; found, 414.1694.

1-(3-(4-(2,3-Dichlorophenyl)piperazin-1-yl)phenyl)-5-oxopyrrolidine-3-carbohydrazide (12b): Brown solid; yield: 70%; m.p.: 144-146 ºC; IR (neat, ν_{max}, cm^{-1}): 3308, 2982, 1668, 1598, 1339; ^{1}H NMR (400 MHz, DMSO-d_6, δ ppm): 9.33 (s, 1H, NH), 7.88 (s, 1H, Ar-H), 7.52 (d, *J* = 8.0 Hz, 1H, Ar-H), 7.39 (t, *J* = 8.2 Hz, 1H, Ar-H), 7.29 (d, *J* = 7.0 Hz, 2H, Ar-H), 7.19 (d, *J* = 7.8 Hz, 1H, Ar-H), 7.11 (d, *J* = 6.0 Hz, 1H, Ar-H), 4.04-3.93 (m, 2H, NH_2), 3.70 (s, 2H, CH_2), 2.90 (s, 8H, $(CH_2)_4$), 2.76-2.69 (m, 1H, CH), 2.64 (dd, *J* = 17.0, 7.1 Hz, 1H, CH), 2.51 (s, 1H, CH); HRMS (ESI) *m/z*: calcd. for $C_{21}H_{23}Cl_2N_5O_2$ $[M + H]^+$ 448.1307; found, 448.1304.

5-Oxo-1-(3-(4-(*p*-tolyl)piperazin-1-yl)phenyl)pyrrolidine-3-carbohydrazide (12c): Brown solid; yield: 76%; m.p.: 140-142 ºC; IR (neat, ν_{max}, cm^{-1}): 3310, 2980, 1661, 1595, 1344; ^{1}H NMR (400 MHz, DMSO-d_6, δ ppm): 7.40 (t, *J* = 8.0 Hz, 1H, Ar-H), 7.20 (d, *J* = 7.4 Hz, 1H, Ar-H), 7.02 (d, *J* = 8.0 Hz, 3H, Ar-H), 6.82 (d, *J* = 8.0 Hz, 3H, Ar-H), 4.13 (s, 2H, NH_2), 4.02-3.95 (m, 1H, CH), 3.89-3.82 (m, 1H, CH), 3.01

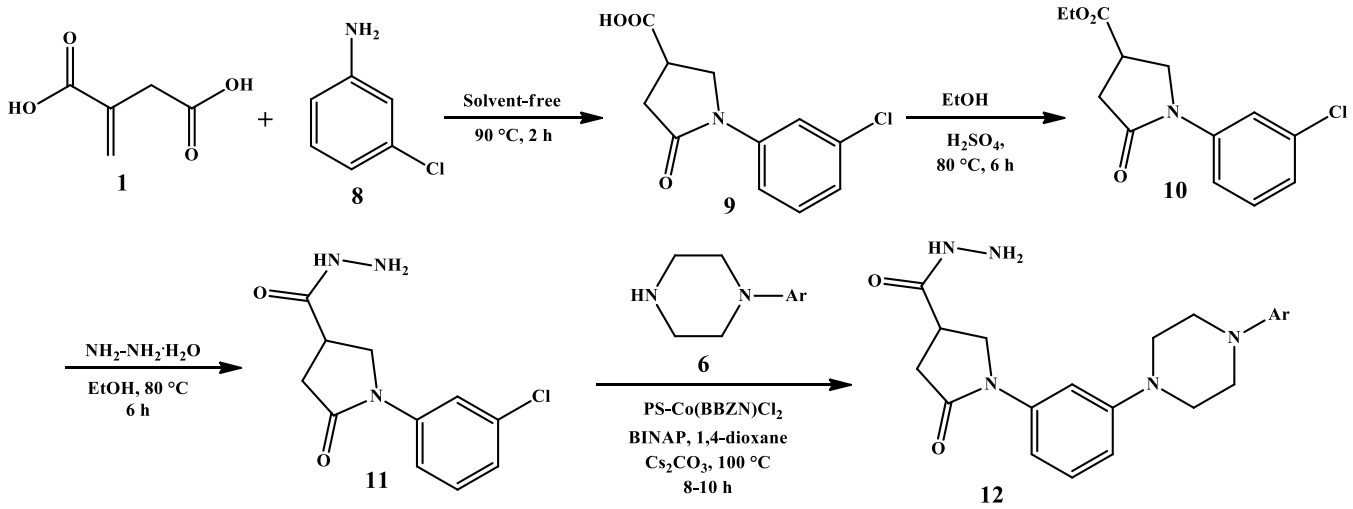

Scheme-II: Synthesis of regioisomeric series of piperazine–pyrrolidone acyl hydrazide hybrids

(s, 8H, $(CH_2)_4$), 2.75 (dd, *J* = 8.0, 6.0 Hz, 1H, CH), 2.65 (dd, *J* = 8.0, 7.2 Hz, 1H, CH), 2.51 (s, 1H, CH), 2.20 (s, 3H, CH_3); HRMS (ESI) *m/z*: calcd. for $C_{22}H_{27}N_5O_2$ $[M + H]^+$ 394.2243; found, 394.2240.

1-(3-(4-(2-Fluorophenyl)piperazin-1-yl)phenyl)-5-oxopyrrolidine-3-carbohydrazide (12d): Brown solid; yield: 68%; m.p.: 150-152 ºC; IR (neat, ν_{max}, cm^{-1}): 3312, 2984, 1666, 1599, 1334; ^1H NMR (400 MHz, DMSO-d_6, δ ppm): 9.35 (s, 1H, NH), 7.88 (s, 1H, Ar-H), 7.61-7.48 (m, 1H, Ar-H), 7.39 (t, *J* = 7.7 Hz, 1H, Ar-H), 7.19 (d, *J* = 7.1 Hz, 1H, Ar-H), 7.14-7.06 (m, 2H, Ar-H), 6.99 (dd, *J* = 8.0, 6.0 Hz, 2H, Ar-H), 3.98 (d, *J* = 8.8 Hz, 1H, CH), 3.76 (s, 2H, NH_2), 3.57-3.50 (m, 1H, CH), 3.19 (dd, *J* = 8.0, 7.1 Hz, 1H, CH), 2.93 (s, 8H, $(CH_2)_4$), 2.77-2.71 (m, 1H, CH), 2.65 (dd, *J* = 8.0, 6.0 Hz, 1H, CH); HRMS (ESI) *m/z*: calcd. for $C_{21}H_{24}FN_5O_2$ $[M + H]^+$ 398.1992; found, 398.1996.

Cell viability assay: The cell viability experiments were conducted by alamar blue assay [14-16]. Briefly, 2×10^3 MCF-7 cells were seeded in 96-well plates, supplemented with 2% FBS maintained at 37 ºC in a humidified 5% CO_2 incubator for 72 h. The compounds at 10-fold serial diluted concentrations (0.001, 0.01, 0.1, 1.0, 10.0 and 100.0 μM) were treated. Following treatment, the cells were placed in an incubator with 0.2 mL of 10% Alamar Blue solution at 37 ºC and 5% CO_2 for 4 h. They were rinsed with PBS. Later, with the help of Tecan microplate reader, fluorescence was measured at an excitation wavelength of 575 nm and an emission wavelength of 595 nm. Dose-response curves were used to determine IC_{50} values. The IC_{50} values for each compound were calculated using GraphPad Prism version 10.0 software (GraphPad Software Inc., San Diego, CA, USA). All measurements were performed in triplicate to ensure the reliability and reproducibility of the results.

Docking studies: Molecular docking studies were carried out using AutoDock Tools version 1.5.7 [17] to estimate the binding contacts and affinity of ligand **7b** within the hydrobhobic groove of 1G5J. The crystal structure 1G5J of the BCL-XL protein complexed with a BAD peptide was obtained from the RCSB Protein Data Bank (PDB ID: 1G5J). Before docking studies, the protein structure was processed by removing crystallographic water molecules and heteroatoms and subsequently adding polar hydrogen atoms to achieve appropriate protonation of the binding site residues during the docking procedure. The molecular structures of the ligands **7b** and NPB were taken and geometrically optimised using Avogadro software [18]. The optimised structures of the ligands were stored in Mol2 format to ensure compatibility with the docking applications used. After preparing the protein and ligand, AutoDock Tools (ADT) was used to set up the docking study. Torsional degrees of freedom were established for the ligands and Kollman charges were assigned to the protein. A docking grid box with dimensions of 60 Å × 60 Å × 40 Å and a grid spacing of 0.375 Å was centered precisely over the hydrophobic groove to encompass all key ligand-protein interactions. Docking simulations utilised the Lamarckian Genetic Algorithm (LGA) with 10 independent runs, allowing for exhaustive conformational sampling to identify the most favourable binding orientations for both protein and inhibitor. All other docking parameters were maintained at default settings to preserve consistency across experimental trials. The binding energy (kcal/mol) were used to rank the obtained binding poses. BIOVIA Discovery Studio Visualizer [19] and UCSF Chimera [20] were used for post-docking analysis to assess hydrogen bonding patterns, binding poses and ligand-protein interactions.

RESULTS AND DISCUSSION

The first series of target compounds, **7a-f**, was synthesised following the synthetic route outlined in **Scheme-I**. The synthesis commenced with the solvent-free reaction of itaconic acid (**1**) and 4-chloroaniline (**2**) at 90 ºC for 2 h, affording 1-(4-chlorophenyl)-5-oxopyrrolidine-3-carboxylic acid (**3**) in 80% yield. Subsequent esterification of compound **3** with ethanol in the presence of conc. H_2SO_4 at 80 ºC for 6 h give ethyl 1-(4-chlorophenyl)-5-oxopyrrolidine-3-carboxylate (**4**) in 90% yield. Treatment of ester **4** with an excess of hydrazine hydrate in ethanol under reflux at 80 ºC for 6 h furnished 1-(4-chlorophenyl)-5-oxopyrrolidine-3-carbohydrazide (**5**) in 83% yield. In the final step, the key intermediate **5** was

coupled with various arylpiperazines (**6**) in 1,4-dioxane at 100 ºC using PS-Co(BBZN)Cl_2 (12 mol%) and BINAP (15 mol%) as catalytic system to afford the desired piperazine–pyrrolidone acyl hydrazide hybrids **7a-f**.

Similarly, a regioisomeric series of piperazine–pyrrolidone acyl hydrazide hybrids (**12a-d**) was synthesized according to **Scheme-II** starting from itaconic acid (**1**) and 3-chloroaniline (**8**). The synthetic sequence proceeded through the isolated intermediates **9**, **10** and **11**, which were obtained in yields of 83%, 86%, and 80%, respectively, before furnishing the final target compounds **12a-d**.

Cytotoxicity activity: The cytotoxicity activities of title compunds **7a-f** and **12a-d** were examined against MCF-7 breast cancer cell lines using alamar blue assay. The IC_{50} values of synthesised compounds and reference drugs are shown in Table-1. It is observed that electron withdrawing chloro (3.10 μM) and fluoro (4.63 μM) groups at *p*- and *o*-position respectively decreased the activity. However, the synergistic effect of these substituents as in compound **7b** increased the potency to 1.46 μM. Introduction of electron withdrawing nitro group at *o*-position almost retained the activity (1.57 μM). On the other hand, electron donating methyl group at *p*-position (3.48 μM) and no subtitution (6.44 μM) reduce the activity. In parallel, incorporation of arylpiperazine moiety to *m*-position was not promising since corresponding compounds **12a-d** showed high IC_{50} values between 3.2 to 39.0 μM. The standard anticancer agents doxorubicin and tamoxifen exhibited IC_{50} values of 0.73 and 1.75 μM, respectively. Importantly, compound **7b** exhibited potent activity with an IC_{50} value of 1.46 μM, making it the most active member of the series. The observed activity was comparable to that of tamoxifen and only approximately two-fold lower than that of doxorubicin, highlighting compound **7b** as a promising lead for further optimization.

TABLE-1
STRUCTURES (Ar), IC_{50} VALUES AND DOCKING SCORES OF TITLE COMPOUNDS

Compd.	Ar	IC_{50} (μM)	Binding score (kcal/mol)
7a	4-ClC_6H_4	3.10	-7.56
7b	2-F-4-ClC_6H_3	1.46	-7.70
7c	2-FC_6H_4	4.63	-6.61
7d	2-$NO_2C_6H_4$	1.57	-7.58
7e	4-MeC_6H_4	3.48	-7.46
7f	C_6H_5	6.44	-6.45
12a	4-ClC_6H_4	3.20	-7.57
12b	2,3-$Cl_2C_6H_3$	3.99	-6.94
12c	4-MeC_6H_4	32.03	-5.41
12d	2-FC_6H_4	39.00	-4.41
Doxorubicin	–	0.73	–
Tamoxifen	–	1.75	–

Docking studies: The optimized 3D structure of compound **7b** is shown in Fig. 1 as a ball-and-stick representation and characterized by aromatic rings and multiple heteroatoms, provides several potential sites for hydrogen bonding and hydrophobic interactions with amino acid residues located within the BCL-XL binding pocket. The 2D interaction profile of

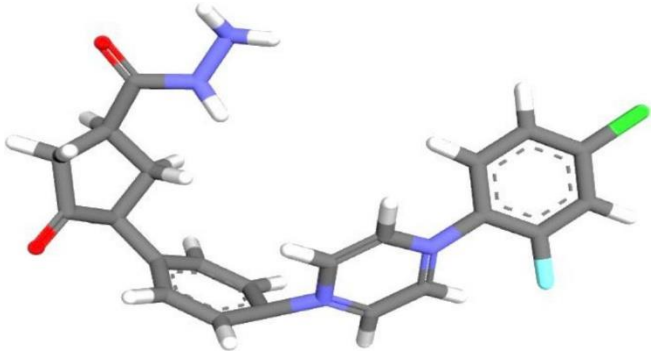

Fig. 1. Optimised 3D-structure of **7b** (in ball and stick model)

compound **7b** with BCL-XL is shown in Fig. 2. Docking analysis revealed the formation of a strong hydrogen bond with ALA203 at a bond distance of 1.92 Å. In addition, π-cation and π-anion interactions were observed with ARG104 and GLU206, respectively. Hydrophobic alkyl and π-alkyl interactions involving residues such as TYR105, ALA97, and ARG104 further contributed to stabilization of the ligand within the binding cavity. Furthermore, π-π stacking interactions with PHE101 played an important role in maintaining the favourable binding orientation of **7b** within the hydrophobic groove.

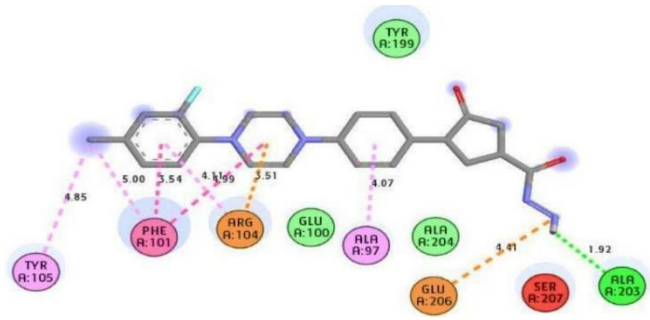

Fig. 2. Two-dimensional interaction map of **7b** with the hydrophobic groove of amino acid residues

The surface representation of the docking complex shown in Fig. 3 illustrates the orientation and accommodation of compound **7b** within the hydrophobic cavity of BCL-XL. The ligand occupied the region responsible for recognition of the BAD peptide and established stable interactions with the surrounding amino acid residues at the protein–protein interaction interface. Fig. 4 depicts the docking pose of compound **7b** (red) within the hydrophobic groove of the BCL-XL protein together with the interacting residues surrounding the binding site. Further analysis of the docking conformation of compound **7b** at the BCL-XL/BAD interface is presented in Fig. 5. In Fig. 5a, the BCL-XL protein is displayed as a blue cartoon structure in complex with the helical BAD peptide segment represented in yellow. Fig. 5b shows the predicted binding orientation of compound **7b** in stick representation within the hydrophobic groove. The superimposed structures presented in Fig. 5c indicate that compound **7b** (red) occupies a binding region similar to that of the previously reported reference ligand NPB (grey) [6]. The docking scores of all synthesized compounds are summarized in Table-1. Among the investigated compounds, **7b** exhibited the highest binding

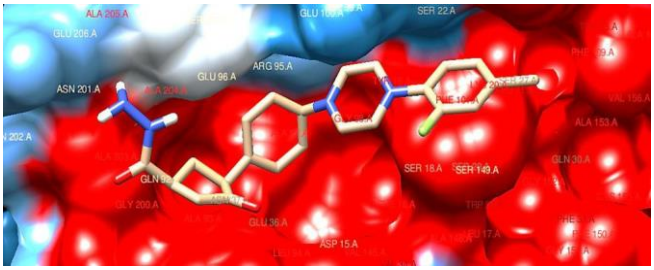

Fig. 3. 3D Surface view of **7b** binding to the hydrophobic groove of BCL-XL (hydrophobic amino acids are shown in red)

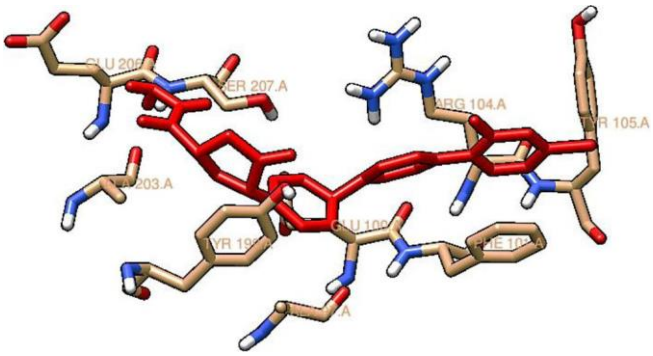

Fig. 4. Docking pose of **7b** within the hydrophobic groove of BCL-XL showing interactions with key surrounding residues

affinity with a docking score of -7.7 kcal/mol, which was comparable to that of the reference ligand NPB (-7.74 kcal/mol).

Conclusion

In conclusion, a series of piperazine–pyrrolidone acyl hydrazide derivatives was successfully synthesized and evaluated for cytotoxic activity against MCF-7 breast cancer cells using the Alamar Blue assay. Among the synthesized compounds, 1-(4-(4-chloro-2-fluorophenyl)piperazin-1-yl)-5-oxopyrrolidine-3-carbohydrazide (**7b**) emerged as the most potent analogue, exhibiting an IC_{50} value of 1.46 μM, which was superior to that of the reference drug tamoxifen (IC_{50} = 1.75 μM). Molecular docking studies provided insights into the possible mechanism underlying the observed anticancer activity. The anti-apoptotic protein BCL-XL is known to inhibit apoptosis through interaction with the pro-apoptotic protein BAD. Docking analysis suggested that compound **7b** binds effectively within the hydrophobic groove of BCL-XL, potentially disrupting the BCL-XL/BAD interaction and thereby promoting apoptotic signaling in cancer cells. These findings highlight compound **7b** as a promising lead candidate for further development as a potential anticancer agent.

ACKNOWLEDGEMENTS

The authors gratefully acknowledge CSIR for providing the JRF fellowship to DN. BBR acknowledges the University of Mysore for the OBC fellowship. HSMY acknowledges the support from the Karnataka Science and Technology Promotion Society (KSTePS), Department of Science and Technology (DST), Government of Karnataka. This work was also supported by the Vision Group on Science and Technology (CESEM) and the Government of Karnataka, India.

CONFLICT OF INTEREST

The authors declare that there is no conflict of interests regarding the publication of this article.

DECLARATION OF AI-ASSISTED TECHNOLOGIES

During the preparation of this manuscript, the authors used an AI-assisted tool(s) to improve the language and no data, results or scientific conclusions were generated by AI. All analyses, interpretations and conclusions are the authors' own. The authors reviewed and edited the content and take full responsibility for the published work.

REFERENCES

1. M. Faizan, R. Kumar, A. Mazumder, N. Salahuddin, N. Kukreti, A. Kumar and M.V.N.L. Chaitanya, *Chem. Biol. Drug Des.*, **103**, e14537 (2024); https://doi.org/10.1111/cbdd.14537

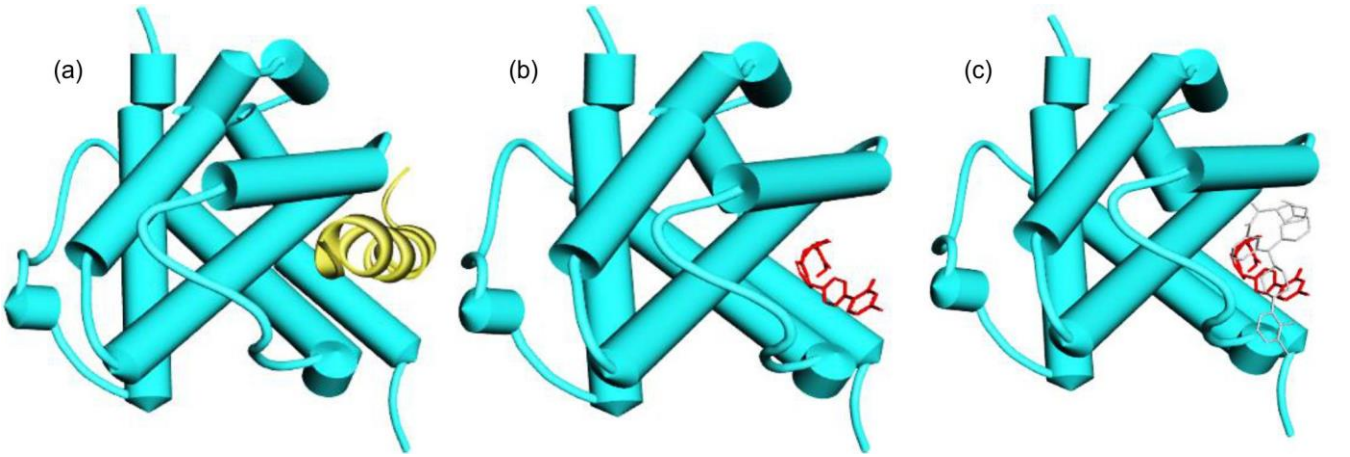

Fig. 5. Docking analysis of **7b** at BCL-XL/BAD interface. (a) The crystal structure 1G5J was taken to model the complex of BCL-XL (blue cartoon) with a 25-residue helical segment of BAD (yellow cartoon); (b) Predicted binding pose of compound **7b** in stick representation binding to a groove within the BCL-XL protein–protein interface; (c) Superimposition of **7b** (red) and NPB (grey) at the hydrophobic groove

2. S. Singh, R. Kumar, S. Tripathi, A. Salahuddin, A. Mazumder and N. Singh, *Chem. Biol. Drug Des.*, **105**, e70077 (2025); https://doi.org/10.1111/cbdd.70077
3. A.A. Bhat, I. Singh, N. Tandon and R. Tandon, *Eur. J. Med. Chem.*, **246**, 114954 (2023); https://doi.org/10.1016/j.ejmech.2022.114954
4. Y. Biliz, B. Hasdemir, H. Başpınar Küçük, M. Zaim, A.M. Şentürk, A. Müdüroğlu Kırmızıbekmez and İ. Kara, *ACS Omega*, **8**, 20073 (2023); https://doi.org/10.1021/acsomega.3c02361
5. A. Ten, R. Koizhaiganova, D. Bissenbay, B. Tursynova, Z. Zhaxibayeva and V. Yu, *ChemistryOpen*, **15**, e202500366 (2026); https://doi.org/10.1002/open.202500366
6. A.-L. Mathieu, O. Sperandio, V. Pottiez, S. Balzarin, A. Herlédan, J. O. Elkaïm, M.-L. Fogeron, C. Piveteau, S. Dassonneville, B. Deprez, B.O. Villoutreix, N. Bonnefoy and F. Leroux, *SLAS Discov.*, **19**, 1035 (2014); https://doi.org/10.1177/1087057114534070
7. N. Rajeev, T.R. Swaroop, S.M. Anil, K.R. Kiran, K.S. Rangappa and M.P. Sadashiva, *J. Chem. Sci.*, **130**, 150 (2018); https://doi.org/10.1007/s12039-018-1540-2
8. T.R. Swaroop, Z.-Q. Wang, Q.Y. Li and H.-S. Wang, *J. Electrochem. Soc.*, **167**, 046504 (2020); https://doi.org/10.1149/1945-7111/ab72ed
9. H.B. Harsha, S. Rangappa, H.D. Preetham, T.R. Swaroop, M. Gilandoust, K.S. Rakesh and K.S. Rangappa, *ChemistrySelect*, **3**, 5228 (2018); https://doi.org/10.1002/slct.201800053
10. S.D. Preethi, K.S. Balaji, D.S. Prasanna, V.H. Kameshwar, J. Shankar, T.R. Swaroop, L. Siddalingaiah and K.S. Rangappa, *Anticancer Agents Med. Chem.*, **17**, 1931 (2017); https://doi.org/10.2174/1871521409666170412120837
11. S.M. Abdel-Wahab, Z.K. Abdelsamii, H.A. Abdel-Fattah, A.S. El-Etrawy, L.N. Dawe, T.R. Swaroop and P.E. Georghiou, *ChemistrySelect*, **3**, 8106 (2018); https://doi.org/10.1002/slct.201801151
12. R. Roopashree, C.D. Mohan, T.R. Swaroop, S. Jagadish and K.S. Rangappa, *Asian J. Pharm. Clin. Res.*, **7**, 309 (2014).
13. Y.H. Lee, S. Lee, J. Sim, E. S. Jo, J.-K. Jung, S. Hyun and J.-H. Kwak, *Bull. Korean Chem. Soc.*, **47**, 333 (2026); https://doi.org/10.1002/bkcs.70101
14. H.M. Poh, Y.S. Chiou, Q.Y. Chong, R.M. Chen, K.S. Rangappa, L. Ma, T. Zhu, A.P. Kumar, V. Pandey, S. Basappa, S.-C. Lee and P. Lobie, *Cancers*, **11**, 1528 (2019); https://doi.org/10.3390/cancers11101528
15. M. Gilandoust, K.B. Harsha, C.D. Mohan, A.R. Raquib, S. Rangappa, V. Pandey, P.E. Lobie, Basappa and K.S. Rangappa, *Bioorg. Med. Chem. Lett.*, **28**, 2314 (2018); https://doi.org/10.1016/j.bmcl.2018.05.020
16. Q.Y. Chong, M.L. You, V. Pandey, A. Banerjee, Y.J. Chen, H.M. Poh, M. Zhang, L. Ma, T. Zhu, S. Basappa, L. Liu and P.E. Lobie, *Oncotarget*, **8**, 74188 (2017); https://doi.org/10.18632/oncotarget.18431
17. D.S. Goodsell, M.F. Sanner, A.J. Olson and S. Forli, *Protein Sci.*, **30**, 31 (2021); https://doi.org/10.1002/pro.3934
18. M.D. Hanwell, D.E. Curtis, D.C. Lonie, T. Vandermeersch, E. Zurek and G.R. Hutchison, *J. Cheminform.*, **4**, 17 (2012); https://doi.org/10.1186/1758-2946-4-17
19. BIOVIA, Dassault Systèmes, Discovery Studio Visualizer, version 21.1.0.20298, Dassault Systèmes: San Diego, CA, USA (2020).
20. E.F. Pettersen, T.D. Goddard, C.C. Huang, G.S. Couch, D.M. Greenblatt, E.C. Meng and T.E. Ferrin, *J. Comput. Chem.*, **25**, 1605 (2004); https://doi.org/10.1002/jcc.20084